ChemComm

COMMUNICATION

View Article Online
View Journal

Cite this: DOI: 10.1039/c9cc00994a

Received 2nd February 2019,
Accepted 29th March 2019

DOI: 10.1039/c9cc00994a

rsc.li/chemcomm

A human vision inspired adaptive platform for one-on-multiple recognition†

Zhiyang Zhu, Jianbin Huang and Yun Yan *

The fluorescence of a coordinative molecule DCM displaying an intramolecular charge transfer (ICT) effect is regulated by several metal ions. These DCM–metal complexes were adopted to recognize different chemicals, including the recognition of triethylenetetramine, thiol-containing amino acids, and H_2S upon binding DCM with Zn^{2+}, Ag^{+}, and Pb^{2+}, respectively. This is in analogy to the general mode of human trichromatic color vision.

Nature has long been a grandmaster in teaching chemists to make complicated functionalities out of the simplest building blocks. One impressive lesson is the trichromatic color vision of human eyes, where one simple pigment of retinal is used to recognize different colors of light (Scheme 1a).[1] Generally, the excited state of retinal is tuned when it binds to different proteins, including red, green, and blue opsins, which enable the recognition of R, G, and B colors on one platform.[2,3] Such a one-on-multiple strategy is commonly utilized by animals. There are numerous evolving opsins and several analogues of retinal, which helped animals to adapt to certain living environments using limited molecules.[4–6]

Inspired by these natural masteries, we believe that the chemical recognition activity can also be designed in a similar way, namely, to achieve diversified recognition on the platform formed by the same molecule. The key point is to design a reporting unit that can non-covalently bind to different recognizing units. However, so far, people have not mastered such an elegant strategy to recognize desired components in an artificial world, and considerable efforts were put into the design of specific detectors for each target.[7–13] Such a 'one-on-one' method will cost too much energy and resources, which is in clear contrast to the smart behavior of retinal in receiving the full spectrum of light.

Beijing National Laboratory for Molecular Sciences (BNLMS), State Key Laboratory for Structural Chemistry of Unstable and Stable Species, College of Chemistry and Molecular Engineering, Peking University, Beijing, 100871, China.
E-mail: yunyan@pku.edu.cn

† Electronic supplementary information (ESI) available. See DOI: 10.1039/c9cc00994a

Herein, we report a 'one-on-multiple' strategy, which resembles the typical mode of human vision generation (Scheme 1b). Starting with a single fluorescent molecule **DCM**, we differentiated three categories of small molecules, including polyamine, thiol-containing amino acids, and H_2S. **DCM** is designed to have a dicyanomethylene-4*H*-pyran-based reporting unit, which is expected to display emission color change in different environments owing to the presence of conjugated donor–acceptor groups. Two coordinating arms were covalently attached to the reporting unit. Upon coordinating to metal ions, the **DCM**–metal complex displayed an emission different from the native **DCM** as a result of the existence of intramolecular charge transfer (ICT) states. Excitingly, each **DCM**–metal system exhibited a specific recognition ability toward a specific chemical, which was accompanied by reversed fluorescence transitions. As a result, starting from the same **DCM** molecule, we can respectively recognize three categories of chemicals mediated by the coordination of three metal ions. This one-on-multiple strategy is in analogy to the human vision generation. We envision that such

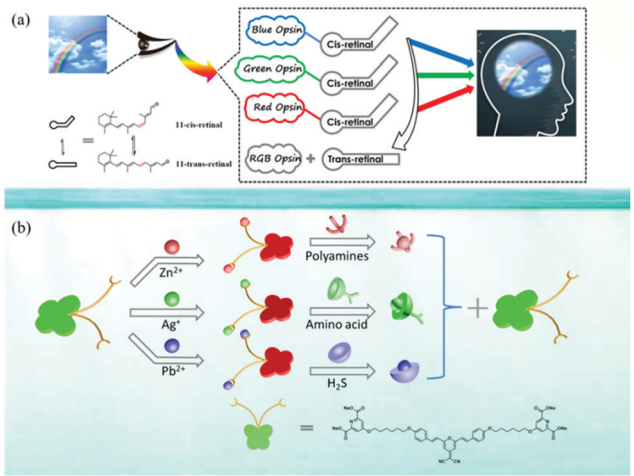

Scheme 1 Illustration of (a) human vision generation and (b) our strategies for the construction of a sensing platform.

a bio-inspired strategy will open up a new horizon for the development of chemical recognition.

DCM is a coordinative amphiphile synthesized in our lab (Scheme S1, ESI†). This molecule has a butterfly-like topology in which two coordinating antennae are attached to a fluorescent core (Scheme 1). According to previous research, phenyl substituted dicyanomethylene-4*H*-pyran displays distinct optical behaviors in different environments due to the interconversion between local excited (LE) states and intramolecular charge transfer (ICT) states.[14,15] Here, the attachment of coordinating arms does not impact its ICT process. As evidence, both the absorption and emission of **DCM** solution can be easily regulated by varying the solvent compositions in water–ethanol mixtures. **DCM** displayed green emission in its good 1–1 (volume ratio) water–ethanol solvent mixture, while red fluorescence was observed in solvents rich in either water or ethanol (Fig. S1a, ESI†). The characteristic red shifts of both absorption maxima (from 560 nm to 630 nm) and emission peaks (rise of a new peak at 499 nm), together with the large Stokes shift indicated the appearance of ICT complexes in water or ethanol rich solvents (Fig. S1b and c, ESI†).[15]

Next, the interaction of **DCM** with different metal ions was explored based on the coordinative ability of the dicarboxylate pyridine head groups. Fig. 1a shows the fluorescence color change of **DCM** in 1–1 water–ethanol mixed solvents upon addition of equivalent (two for Ag^+, Fig. S2, ESI†) metal ions. Notably, the emission color of **DCM** exhibited dramatic changes after addition of Ca^{2+}, Zn^{2+}, Pb^{2+} and Ag^+. FT-IR measurements confirm that these metal ions have coordinated to the dicarboxylate pyridine head (Fig. S3, ESI†). Spectra examination reveals (Fig. 1b and c) new absorption maxima near 500 nm and new emission peaks at around 650 nm, verifying the appearance of ICT states under these conditions.

The coordination triggered red emission is drastically different from the green emission of **DCM** itself. Since metal ions can bind to different molecules respectively, these **DCM**–metal complexes can be further used as individual species for specific recognition purpose. In principle, any material that can remove metal ions from **DCM** will induce a reversed fluorescence

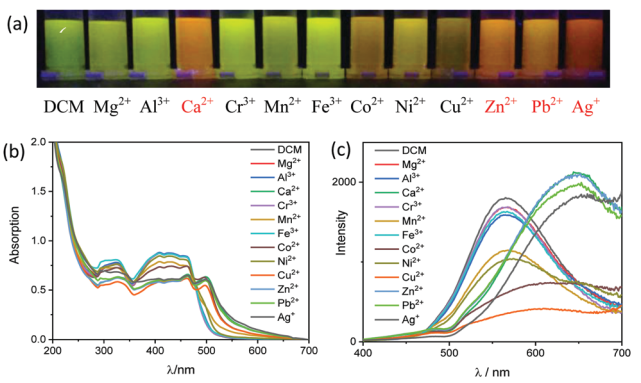

Fig. 1 (a) Fluorescence pictures of **DCM**–M^{n+} systems in 1–1 (volume ratio) water–ethanol mixed solvents under a 365 nm UV lamp. [**DCM**] = [M^{n+}] = [Ag^+]/2 = 50 μM. (b) Absorption spectra and (c) emission spectra of **DCM**–M^{n+} systems in 1–1 water–ethanol mixed solvents.

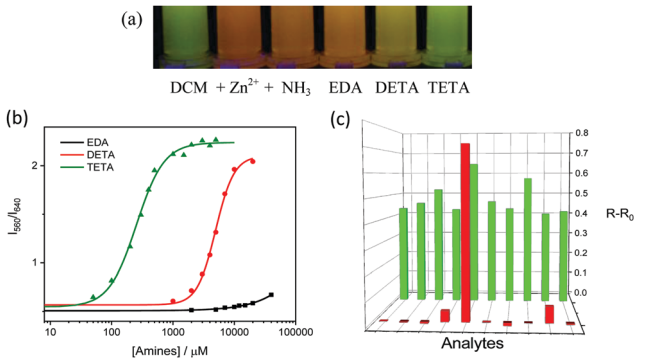

Fig. 2 (a) Fluorescence pictures of **DCM**–Zn^{2+} systems with polyamines in 1–1 (volume ratio) water–ethanol mixed solvents under a 365 nm UV lamp. [**DCM**] = [Zn^{2+}] = 50 μM, [NH_3] = 2 [EDA] = 3 [DETA] = 4 [TETA] = 5 mM. (b) Ratiometric titration of **DCM**–Zn^{2+} upon the addition of polyamines. The I_{560}/I_{640} ratios were plotted as a function of polyamine concentrations. (c) Ratiometric response of **DCM**–Zn^{2+} towards TETA without (red bars) or with (green bars) additional competing species. From left to right: none, NH_3, EDA, DETA, TETA, Et_3N, C_6NH_2, H_2NNH_2, S^{2-}, CO_3^{2-}. [**DCM**] = [Zn^{2+}] = 50 μM, [analytes] = 500 μM.

change in the corresponding **DCM**–metal system. This provided us the fundaments to construct a multiple recognition platform based on one single fluorescent molecule **DCM**. Though most small molecules failed to destruct the **DCM**–Ca^{2+} system, we succeeded in other three systems.

Triethylenetetramine (TETA) is an orphan drug that has been commonly used in the treatment of Wilson's disease for decades.[16] Recent studies also revealed its potential uses in cancer chemotherapy and other diseases.[17–19] However, clinical applications and pharmacological studies of TETA are greatly hindered by the lack of versatile analytical methods, as current protocols for TETA detection are majorly based on chromatography or labelling reagents.[20,21] Here, we achieved direct fluorescence detection of TETA using the **DCM**–Zn^{2+} system. Upon addition of 0.5 mM TETA to 50 μM **DCM**–Zn^{2+} solution, a red-to-green fluorescence transition can be observed (Fig. 2a). Using the fluorescence titration method, we can achieve quantitative detection of TETA in the concentration range of 50–500 μM (Fig. 2b), which covers the commonly used concentrations in preclinical studies.[22] Notably, its analogues including ethylenediamine (EDA) and diethylenetriamine (DETA) only show limited influence on the **DCM**–Zn^{2+} system. At equivalent concentration, the co-existence of EDA or DETA is negligible and doesn't significantly affect the detection of TETA (Fig. 2b and Fig. S4, ESI†). Besides, other competing species such as S^{2-} and CO_3^{2-} or the presence of other metal ions show ignorable influence (Fig. 2c and Fig. S5, ESI†). This desirable selectivity of **DCM**–Zn^{2+} towards TETA can be related to the octahedral coordination configuration usually adopted by Zn^{2+}, which favors the formation of planar chelating structures with multi-dental ligands.

Recognition of specific amino acid has always been an interesting topic in fluorescence sensing area. Among them, most efforts were dedicated to the selective detection of thiol-containing ones, such as cysteine (Cys) and glutathione (GSH),[23–25] due to their crucial role in many physiological aspects.[26,27]

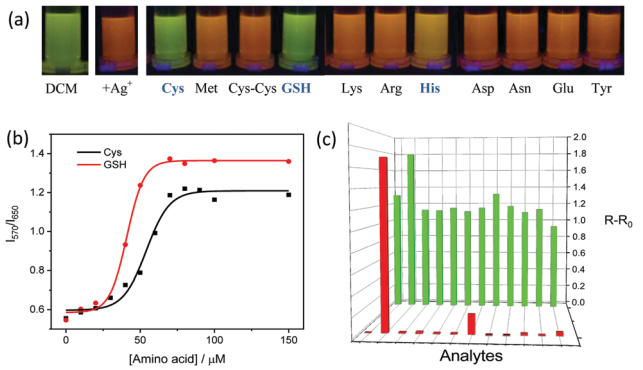

Fig. 3 (a) Fluorescence pictures of **DCM**–Ag^+ systems with polar amino acids in 1–1 (volume ratio) water–ethanol mixed solvents under a 365 nm UV lamp. (b) Ratiometric titration of **DCM**–Ag^+ upon the addition of Cys and GSH. The I_{570}/I_{650} ratios were plotted as a function of amino acid concentrations. (c) Ratiometric response of **DCM**–Ag^+ towards thiol-containing amino acid Cys without (red bars) or with (green bars) various competitors. From left to right: none, Cys, Cys–Cys, Met, Lys, Arg, His, Asp, Asn, Glu, Tyr, BSA (bovine serum albumin). [**DCM**] = $[Ag^+]/2$ = 50 μM, [amino acids] = 100 μM if not mentioned.

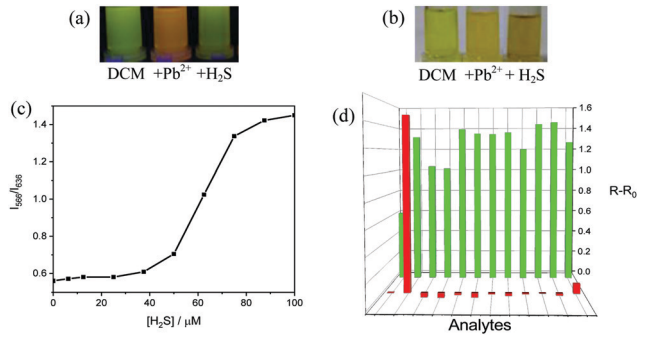

Fig. 4 (a) Fluorescence pictures of **DCM**–Pb^{2+} systems in the presence of H_2S in 1–1 water–ethanol mixed solvents under a 365 nm UV lamp. (b) Optical pictures of **DCM**–Pb^{2+} systems in the presence of H_2S. [**DCM**] = $[Pb^{2+}]$ = 50 μM, $[H_2S]$ = 150 μM. (c) Ratiometric titration of **DCM**–Pb^{2+} upon the addition of H_2S. The I_{566}/I_{636} ratios were plotted as a function of H_2S concentrations. (d) Ratiometric response of **DCM**–Pb^{2+} towards H_2S against other competitors (red bars) and the response of **DCM**–Pb^{2+} in the presence of competitors towards H_2S (green bars). From left to right: none, S^{2-}, F^-, Cl^-, Br^-, I^-, CO_3^{2-}, $C_2O_4^{2-}$, SO_4^{2-}, PO_4^{3-}, and CH_3COO^-.

Here, we achieved discrimination of Cys and GSH from other amino acids based on the high affinity of Ag^+ to thiol groups. On the addition of 1 equivalent of Cys or GSH, the red fluorescence of the **DCM**–Ag^+ system turned green immediately. As indicated by the ratiometric signal, quantitative detection of Cys and GSH is viable in the concentration range of 30–70 μM with a detection limit of 20 μM (Fig. 3b). Other types of amino acids bearing coordinating groups, such as carboxyl groups, hydroxyl groups, amino groups and guanidine groups, show limited interferences (Fig. 3c) and do not significantly affect the detection of Cys and GSH (Fig. S6, ESI†). Basically, the selectivity of Ag^+ to thiol containing amino acids can be explained by HSAB theory, where the thiol group is a soft base, and Ag^+ is a soft acid.[28]

Hydrogen sulfide (H_2S) has been regarded as a toxic gas for a long time.[29] However, recent studies revealed that H_2S also plays some important roles in biological systems,[30] therefore the detection of the H_2S level in solution in the biosystem has attracted intensive interest.[31–34] Herein, the **DCM**–Pb^{2+} system was proved to be optimizing for the selective detection of H_2S. Upon addition of 150 μM H_2S to the solution, the red bright fluorescence of the **DCM**–Pb^{2+} system turned dark green (Fig. 4a), accompanied by the darkening of solution color (Fig. 4b). In the fluorescence titration curve, there was a sharp increase of the ratiometric signal when the concentration of H_2S exceeded 30 μM (Fig. 4c), and quantitative detection is viable in the concentration range of 40–100 μM. This detection ability is comparable to some previously reported H_2S fluorescent sensors.[33,34] Significantly, the existence of other coordinative species, such as I^-, CO_3^{2-}, SO_4^{2-}, HPO_4^{2-}, and GSH, does not significantly affect the detection of H_2S using **DCM**–Pb^{2+} complex (Fig. 4d and Fig. S7, ESI†), indicating the specificity of the **DCM**–Pb^{2+} system toward H_2S.

In summary, we demonstrated a facile strategy to develop a one-on-multiple molecular recognition platform based on the combination of one fluorescent amphiphile **DCM** and metal ions. Upon coordinating with metal ions, **DCM** exhibited a huge red-shift of fluorescence color in comparison to itself. This regulation was reversible when metal ions were extracted from DCM–metal complexes. Because each metal ion may have specific binding affinity to different chemicals resulting in the recovery of the **DCM** emission, the **DCM**–metal system is able to recognize different chemicals. We verified that it is possible to discriminate TETA, Cys and GSH, and H_2S using **DCM**–Zn^{2+}, **DCM**–Ag^+, and **DCM**–Pb^{2+}, respectively. This is very similar to the way that human eyes recognize red, green, and blue colors with the same retinal molecule when it binds to red, green, and blue opsins. Such a bio-inspired strategy will open up a new horizon in the design of an adaptive platform for versatile chemical recognition.

This work was financially supported by the National Natural Science Foundation of China (NSFC, Grant No. 91856120, 21573011, and 21633002) and the Ministry of Science and Technology of China (2017YFB0308800).

Conflicts of interest

There are no conflicts to declare.

Notes and references

1 G. J. Wald, *Science*, 1964, **145**, 1007–1016.
2 J. Nathans, *Biochemistry*, 1990, **29**, 9746–9752.
3 K. Fujimoto, J.-y. Hasegawa, S. Hayashi, S. Kato and H. Nakatsuji, *Chem. Phys. Lett.*, 2005, **414**, 239–242.
4 P. W. Lucas, B. W. Darvell, P. K. D. Lee, T. D. B. Yuen and M. F. Choong, *Folia Primatol.*, 1998, **69**, 139–152.
5 H. Siitari, J. Honkavaara and J. Viitala, *Proc. R. Soc. London, Ser. B*, 1999, **266**, 2125–2129.
6 J. N. Lythgoe, *Vision Res.*, 1984, **24**, 1539–1550.
7 D. Ding, K. Li, B. Liu and B. Z. Tang, *Acc. Chem. Res.*, 2013, **46**, 2441–2453.
8 L. Yuan, W. Y. Lin, K. B. Zheng and S. S. Zhu, *Acc. Chem. Res.*, 2013, **46**, 1462–1473.
9 S. W. Thomas III, G. D. Joly and T. M. Swager, *Chem. Rev.*, 2007, **107**, 1339–1386.

10 L. E. Kreno, K. Leong, O. K. Farha, M. Allendorf, R. P. Van Duyne and J. T. Hupp, *Chem. Rev.*, 2012, **112**, 1105–1125.
11 Y. Liu, X. Dong and P. Chen, *Chem. Soc. Rev.*, 2012, **41**, 2283–2307.
12 K. Hisataka, O. Mikako, A. Raphael, P. L. Choyke and U. Yasuteru, *Chem. Rev.*, 2010, **110**, 2620–2640.
13 M. Vendrell, D. Zhai, J. C. Er and Y. T. Chang, *Chem. Rev.*, 2012, **112**, 4391–4420.
14 H. Tong, Y. Hong, Y. Dong, Y. Ren, M. Häussler, J. W. Y. Lam, K. S. Wong and B. Z. Tang, *J. Phys. Chem. B*, 2007, **111**, 2000–2007.
15 X. F. Xu, R. Q. Zhang, Z. X. Cao and Q. E. Zhang, *J. Theor. Comput. Chem.*, 2008, **7**, 719–736.
16 A. Ala, A. P. Walker, K. Ashkan, J. S. Dooley and M. L. Schilsky, *Lancet*, 2007, **369**, 397–408.
17 J. Liu, L. Guo, F. Yin, X. Zheng, G. Chen and Y. Wang, *Biomed. Pharmacother.*, 2008, **62**, 480–485.
18 L. Wang, X. Luo, C. Li, Y. Huang, P. Xu, L. H. Lloyd-Davies, T. Delplancke, C. Peng, R. Gao, H. Qi, C. Tong and P. Baker, *Oxid. Med. Cell. Longevity*, 2017, 3481710.
19 G. J. S. Cooper, *Drugs*, 2011, **71**, 1281–1320.
20 A. Othman, J. Lu, T. Sunderland and G. J. S. Cooper, *J. Chromatogr. B: Anal. Technol. Biomed. Life Sci.*, 2007, **860**, 42–48.
21 J. Lu, Y. K. Chan, S. D. Poppitt and G. J. S. Cooper, *J. Chromatogr. B: Anal. Technol. Biomed. Life Sci.*, 2007, **859**, 62–68.
22 J. Lu, *Mol. Cancer Ther.*, 2010, **9**, 2458–2467.
23 W. Li, L. Long, L. Yuan, Z. Cao, B. Chen and W. Tan, *Org. Lett.*, 2008, **10**, 5577–5580.
24 X. Yang, Y. Guo and R. M. Strongin, *Angew. Chem., Int. Ed.*, 2011, **50**, 10690–10693.
25 W. Hao, A. McBride, S. McBride, J. P. Gao and Z. Y. Wang, *J. Mater. Chem.*, 2011, **21**, 1040–1048.
26 X. F. Wang and M. S. Cynader, *J. Neurochem.*, 2000, **74**, 1434–1442.
27 S. Shahrokhian, *Anal. Chem.*, 2001, **73**, 5972–5978.
28 R. G. Pearson, *J. Am. Chem. Soc.*, 1963, **85**, 3533–3539.
29 C. Wang, X. Chu and M. Wu, *Sens. Actuators, B*, 2006, **113**, 320–323.
30 O. Kabil and R. Banerjee, *J. Biol. Chem.*, 2010, **285**, 21903–21907.
31 C. Liu, J. Pan, S. Li, Y. Zhao, L. Y. Wu, C. E. Berkman, A. R. Whorton and M. Xian, *Angew. Chem., Int. Ed.*, 2011, **50**, 10327–10329.
32 S. K. Bae, C. H. Heo, D. J. Choi, D. Sen, E. H. Joe, B. R. Cho and H. M. Kim, *J. Am. Chem. Soc.*, 2013, **135**, 9915–9923.
33 Z. Du, B. Song, W. Zhang, C. Duan, Y. L. Wang, C. Liu, R. Zhang and J. Yuan, *Angew. Chem., Int. Ed.*, 2018, **57**, 3999–4004.
34 J. Hong, W. Feng and G. Feng, *Sens. Actuators, B*, 2018, **262**, 837–844.

